Uptake kinetics of spontaneously emulsified microdroplets at an air–liquid interface

Léa Delance, Charlotte Veillon, Nicolas Passade-Boupat, François Lequeux, Laurence Talini, Emilie Verneuil

Uptake kinetics of spontaneously emulsified microdroplets at an air-liquid interface†

Léa Delance,[abc] Charlotte Veillon,[ab] Nicolas Passade-Boupat,[cd] François Lequeux,[ab] Laurence Talini,[*e] and Emilie Verneuil[ab]

Understanding the transfers occurring at the interfaces between emulsions and air is required to predict the properties of foamed emulsions, used for example as antifoaming lubricants or for oil extraction. Whereas bubbling oil-in-water emulsions have been studied in details, oil-in-oil emulsions have received less attention. We consider a phase-separating mixture of three oils being Polydimethylsiloxane (PDMS), decane and cyclopentanol. PDMS is dispersed as submicrometer-sized droplets by spontaneous emulsification. In bulk, we show that the time evolution of the emulsion is driven by undelayed coalescence of the Brownian microdroplets. At the freshly created interface of an air bubble created in the emulsion, we use tensiometry measurements to investigate the uptake kinetics of PDMS-rich microdroplets at the air-liquid interface. Specifically, we evidence two mechanisms of uptake: the advection of droplets at the interface during bubble swelling, followed by their diffusion on a longer time scale. We model the growth of the PDMS-rich layer at the interface and, finally, we establish the surface energy of a thin film of PDMS-rich phase squeezed between air and liquid as a function of its thickness.

1 Introduction

The stability of foams is greatly enhanced by the addition to the liquid of surfactants or, as increasingly used, of colloidal particles, resulting in the formation of Pickering foams[9]. Along another line, foaming of emulsions has been recently considered[20,21]. Foamed emulsions consist of air bubbles dispersed in a continuous liquid phase containing microdroplets of an immiscible liquid and of typical size much smaller than the bubble size[20,21]. Over time, the stability of these foams depends on the transport mechanisms and coalescence of the droplets both in the bulk and with the air interface[15]. Most studies in the literature focus on oil-in-water emulsions stabilized by surfactants[16,18]. Depending on the oil fraction, droplet size or surfactant type, the emulsified phase has a stabilising or destabilising effect on the foam. From a practical perspective, controlling foam destabilisation is of particular interest in the field of antifoaming additives. These additives consist of liquids that are immiscible with the continuous liquid phase, dispersed as microdroplets, and cause foam films to break by entering the air-liquid interface[1,6,7,12]. PDMS droplets are often used for their antifoaming properties because the low surface tension of PDMS favours their emergence at the air interface.

Two physical parameters have been introduced to describe droplet entry at an air-liquid interface[6]. The entry coefficient is defined as $E = \gamma_{a-l} + \gamma_{l-d} - \gamma_{d-a}$, where γ_{i-j} represents the surface tension between fluids i and j, the indices a, l, and d standing for air, liquid and dispersed phase respectively. E compares the total interfacial energy when the dispersed phase spreads at the air interface versus remains dispersed in the liquid. Hence, when E is positive, it is energetically favorable for droplets dispersed in the bulk to enter the air-liquid interface. However, this simple energetic point of view has been supplemented by an entry energy barrier which may hinder the coalescence of the antifoaming droplets with the air interface. This barrier characterises the stability of the thin liquid film squeezed between the air bubble and dispersed droplets as they migrate towards the bubble interface. The stability of this film is then related to its disjoining pressure and was shown to be controlled, in the case of aqueous foams, by addition of surfactants[19]. The entry of droplets at the air interface is allowed if the latter thin film breaks.

Antifoam mechanisms have been scarcely studied in the case of non-aqueous liquids without surfactants whereas oil-in-oil emulsions are commonly used as lubricants, with the dispersed phase acting as an antifoam[4]. In this paper, we offer to describe the transport mechanisms governing the coalescence of emulsion microdroplets with a newly created air interface. For this purpose, we use a ternary mixture of oils that spontaneously emulsifies, thereby allowing for a fine control of the sub-micrometer sized dispersed droplets. On the one hand, we observe the coalescence of the microdroplets in the bulk that we model. On the other hand, we study the time evolution of the newly created interface between air and emulsion at which microdroplets of the dispersed phase spread.

2 Material and Methods

To create emulsified microdroplets of PDMS, we take advantage of spontaneous emulsification that appears when liquids of different solubility are brought into contact - also called Ouzo effect. For example, mixing a solution of ethanol and anethol with water causes spontaneous emulsification since anethol is miscible with ethanol but not with water[24]. Here, we use a ternary system composed of Polydimethylsiloxane (PDMS, trimethylsiloxy terminated, viscosity 60 000 cSt, from ABCR), cyclopentanol (purity>99%, from Sigma-Aldrich) and decane (purity>99%, from GPR Rectapur). Decane is fully miscible with cyclopentanol and PDMS, whereas PDMS and cyclopentanol are only partially mis-

0[a] *Soft Matter Sciences and Engineering (SIMM), ESPCI Paris, PSL University, Sorbonne Université, CNRS, F-75005 Paris, France*

0[b] *Laboratoire Physico-Chimie des Interfaces Complexes, ESPCI Paris, 10 rue Vauquelin, F-75231 Paris, France*

0[c] *TOTALEnergies S.A., Pôle d'Etudes et de Recherches de Lacq, BP 47, 64170 Lacq, France*

0[d] *Laboratoire Physico-Chimie des Interfaces Complexes, Chemstartup, RD 817, 64170 Lacq, France*

0[e] *CNRS, Surface du Verre et Interfaces, Saint-Gobain, 93300 Aubervilliers, France. E-mail: laurence.talini@cnrs.fr*

0† Electronic Supplementary Information (ESI) available. See DOI: 10.1039/cXsm00000x/

cible. Therefore, when these three liquids are mixed, either a monophasic or biphasic solution is formed. The mixture's phase diagram can be found in the Supplementary information†. In our study, we remain in the biphasic domain which corresponds to cyclopentanol mass fractions larger than $57\% \pm 1\%$. In this case, the solution is composed of a PDMS-poor continuous phase and a PDMS-rich dispersed phase. In the following, the PDMS-poor phase, which is mostly a cyclopentanol/decane mixture, will be referred to as the oil mixture.

We prepare two series of mixtures: firstly, cyclopentanol mass fraction in the oil mixture is varied from 60% to 95% with an added PDMS mass fraction set to $\Phi_{PDMS} = 400$ ppm. Secondly, the cyclopentanol mass fraction is set to either 70% or 80%, and the PDMS fraction is varied between 10 ppm and 1500 ppm. In the latter series, Dynamic Light Scattering (ALV/CGS-3) experiments performed right after mixing the three liquids showed that autoemulsification always occurs. As a result, the solubility c of PDMS in the oil mixture is necessarily much smaller than the smallest fraction tested (10 ppm), which provides an estimate for $c = 1$ ppm.

We measured the composition of the PDMS-rich phase by volumetric measurement. To do so, we gently poured a controlled volume of oil mixture over PDMS, and waited for the equilibrium between the two phases to be reached for typically 2 months. By pouring 5 mL of an oil mixture with a cyclopentanol and decane mass fraction of respectively 70% and 30% over 1.3 mL of PDMS, we found that the volume of the latter phase increased until 2.2 mL. This means that the volumic fraction of PDMS in the PDMS-rich phase is $60\% \pm 1\%$. We could not determine the cyclopentanol nor decane volume fraction in this phase. However, we expect a small concentration in cyclopentanol in the PDMS-rich phase, since cyclopentanol is only partially miscible with PDMS. Therefore, we assume the PDMS-rich dispersed phase is composed of 60% of PDMS and 40% of decane in volume. Thus, in the following, the droplet volume fraction ϕ_0 will be determined from the introduced PDMS mass fraction Φ_{PDMS} through:

$$\phi_0 = \frac{\Phi_{PDMS}}{\Phi_{PDMS} + \frac{d_{PDMS}}{d_l}(1 - \Phi_{PDMS})} \frac{1}{0.6}, \qquad (1)$$

where d_l is the continuous phase density and d_{PDMS} the PDMS density. Here, the densities of all mixtures were computed within the approximation of volume additivity from the pure liquid values reported in the Supplementary information†. Assumption is made that, in our experiments, the transfer of oil mixture through evaporation is negligible.

The three interfacial tensions between oil mixture l, air a and dispersed phase d were measured using a rising drop or bubble tensiometer (Teclis). All experiments were performed at constant temperature of 295.0 ± 0.5 K. For a cyclopentanol mass fraction of 70%, we find: $\gamma_{l-a} = 26.9 \pm 0.1$ mN/m, $\gamma_{d-a} = 21.7 \pm 0.1$ mN/m and $\gamma_{l-d} = 0.8 \pm 0.7$ mN/m. The interfacial tension γ_{l-d} between the oil mixture and dispersed phase exhibits a large uncertainty for two reasons. Firstly, density is an input parameter in tensiometry: the exact composition of the phases being unknown, uncertainties based on the densities of the phases are large. Secondly, the interfacial tension being small, it is close to the tensiometer accuracy.

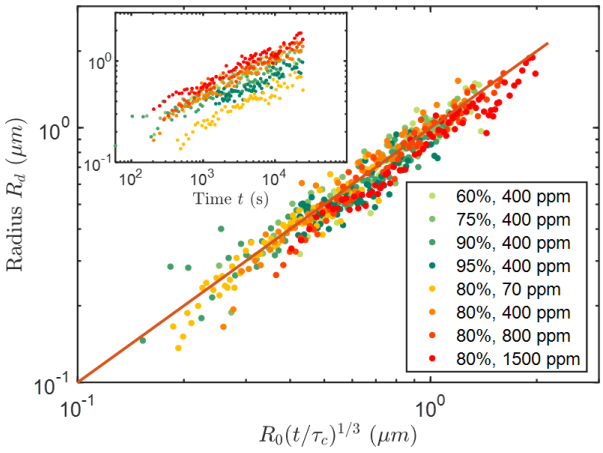

Fig. 1: Time-dependent measured radius R_d of autoemulsified microdroplets as a function of computed radius from Eq. 4. Ternary mixture: cyclopentanol/decane/PDMS with different mass fractions in cyclopentanol (in %) and in PDMS (in ppm). The microdroplets are composed of a PDMS-rich phase and are dispersed in a cyclopentanol/decane mixture with traces of PDMS. Inset: Measured radius R_d as a function of time.

The viscosities η of each decane/cyclopentanol mixtures according to their mass fractions were also measured with a rheometer (Low Shear 400, Lamy rheology). The results are reported in the Supplementary information†. The addition of PDMS in small amounts (less than 0.2% of total mass) is assumed not to change the viscosity.

To prepare the emulsions, PDMS is first diluted in decane - with which it is fully miscible - and this mixture is then added to cyclopentanol - with which PDMS is only partially miscible - under gentle agitation for 10 seconds. Autoemulsification of a PDMS-rich phase spontaneously occurs, which is monitored over time by Dynamic Light Scattering (ALV/CGS-3) and the CONTIN algorithm[17]. This allows us to measure the time variations of the microdroplet radius of the dispersed phase.

3 Time evolution of autoemulsified microdroplets within the bulk

We first characterise the microdroplets' behavior within the bulk emulsion immediately after the autoemulsification process has started. The variation of microdroplet radius with time is shown in Fig. 1 (Inset) for two series of mixtures. First, the cyclopentanol over decane mass fraction was varied between 60% and 95% with a constant 400 ppm PDMS concentration (light to dark green). Second, the cyclopentanol-decane mass fraction was set to 80% and the PDMS ratio was increased from 70 to 1500 ppm (yellow to red). In all mixtures, the radius increases according to a power law. Meanwhile, the width of the radius distribution (not shown) remains smaller than 10% of the average radius, evidencing the emulsions are rather monodisperse. Two mechanisms can explain the droplet growth: Ostwald ripening and the coalescence of droplets due to Brownian motion. Since PDMS is nearly insoluble in the oil mixtures, Ostwald ripening is likely to be negligible

and we first test the growth law due to coalescence.

The coalescence of Brownian droplets right after collision has been described theoretically[2,23] and the radius of droplets is expected to vary with time as

$$R_d = R_0 \left(1 + \frac{t}{\tau_c}\right)^{1/3}, \quad (2)$$

where R_0 is the radius of the droplets at time $t = 0$, and

$$\tau_c = \frac{2\pi\eta R_0^3}{k_B T \phi_0}, \quad (3)$$

where η the viscosity of the continuous liquid phase, $k_B T$ the thermal energy, and ϕ_0 is the droplet volume fraction, assumed here to be constant and homogeneous. An estimate of τ_c yields $\tau_c \sim 200$ s so that the approximation $1 << t/\tau_c$ holds. In this limit, Eq. 2 is reduced to:

$$R_d \simeq R_0 \left(\frac{t}{\tau_c}\right)^{1/3}. \quad (4)$$

We plot the experimental radius as a function of the predicted radius from Eq. 4 in Fig. 1. Remarkably, all data collapse onto the $y = x$ line. The excellent agreement between the experimental data and the prediction demonstrates that the microdroplet growth can be described by a mechanism of diffusion-limited coalescence, regardless of the composition of the oil mixture. In the following, we offer to check that this mechanism overcomes ripening, i.e. growth of droplets by molecular diffusion, through the continuous phase, of the dispersed phase from smaller droplets. In the literature, the growth rate of droplets undergoing Ostwald ripening has been studied[11] and follows the same equation as the one for coalescence Eq. 2, but with a different time scale denoted τ_{OR}, where:

$$\tau_{OR} = \frac{9 k_B T R_0^3}{8\gamma_{d-l} v_m c D}, \quad (5)$$

with v_m the molecular volume of the disperse phase, c its solubility and D the diffusion coefficient of its molecules in the continuous phase. Using the maximum value estimated for the solubility, $c =$ 1 ppm, the ratio of the characteristics times of Ostwald ripening τ_{OR} versus coalescence τ_c verifies $\tau_{OR}/\tau_c > 20$.

Therefore, the effect of Ostwald ripening can be neglected, and the growth of the autoemulsified droplets is governed by diffusion-limited coalescence. This result also shows that there is no mechanism delaying or hindering droplet coalescence in oil: they coalesce immediately after collision.

4 Transport mechanisms at a freshly created gas interface

4.1 Results

We then focus on the time evolution of a freshly created air interface in the emulsion. To do so, we offer to measure the time variation of the surface tension of a bubble created at the tip of a needle in an autoemulsified ternary mixture of known age. Surface tensions smaller than the oil mixture/air value indicate that a PDMS-rich layer has spread over the bubble and is continuous. This is consistent with the positive value obtained for the spreading parameter $S = \gamma_{l-a} - \gamma_{l-d} - \gamma_{d-a} \simeq +4.4 \pm 0.7$ mN/m: the PDMS-rich phase completely wets the air/liquid interface. This is further confirmed by independent experiments in which droplets of the PDMS-rich phase were deposited on a decane/cyclopentanol bath. They were observed to rapidly spread at the surface of the liquid bath and form a sub-micrometric layer, as confirmed by the presence of colours due to light interferences. In contrast, oil[14] or water[22] droplets deposited at the free surface of respectively water and oil are observed to float on the surface.

Here, we choose to set the mass fraction of cyclopentanol in the oil mixture to 70% and to vary the mass fraction of PDMS. The bubble volume is set to 4 μL, which corresponds to a radius of 1 mm. Before each measurement, ten bubbles are expelled quickly (in 12 seconds) to ensure that the initial air interface at the end of the needle is a fresh air/oil mixture interface. The bubble is then swollen in 1 second. The process is schematized in Fig. 2a.

Results of surface tension measurements over time are shown in Fig. 3a for different PDMS mass fractions. Firstly, a decrease of surface tension is observed until a plateau is reached after several hours. Secondly, for small PDMS fractions (50 and 100 ppm), the initial surface tension corresponds to that of the pure decane/cyclopentanol mixture with air $\gamma_{a-l} = 26.9$ mN/m, as shown by the dotted line in Fig. 3a. This confirms that the air bubble initially exhibits a pure air/oil interface for these small PDMS fractions, and subsequently, microdroplets (composed of 60% in volume of PDMS) diffuse, meet the interface, and spread over it, forming a thin PDMS-rich layer at the bubble surface: this causes the surface tension to decrease. Thirdly, at larger PDMS fractions, the initial bubble surface tension decreases as PDMS mass fraction increases, thereby demonstrating that the PDMS-rich phase has already spread over the bubble interface during swelling. Microdroplets capture during bubble swelling is promoted by advection due to the extensional flow in the liquid created by bubble growth (see Fig. 2 a-c). For this advection transport to be relevant, it should be faster than bubble swelling. PDMS transport to the air interface by advection is expected to increase with PDMS mass fraction. This is in agreement with the observed decrease of initial surface tension as PDMS mass fraction increases. Moreover, observation of a plateau at short times suggests that microdroplets spread quasi-instantaneously at the surface once captured. After this initial bubble swelling step, the thickness of the PDMS-rich layer at the bubble interface further increases by diffusion of the Brownian droplets.

4.2 Discussion

4.2.1 Model for the growth of the PDMS-rich layer

This two-step advection-diffusion mechanism is now modelled to account for the time-dependence of thickness h of the PDMS-rich layer at the surface of the bubble. As depicted in Fig. 2, h is the sum of two contributions, the advection of droplets towards the air/oil interface h_{adv}, and the diffusion of droplets h_{dif}.

Firstly, transport by advection is modelled (Fig. 2 a-c). We consider that all the fluid particles initially located at a distance d_i from the initial disk-shaped air/oil interface will be moved, after

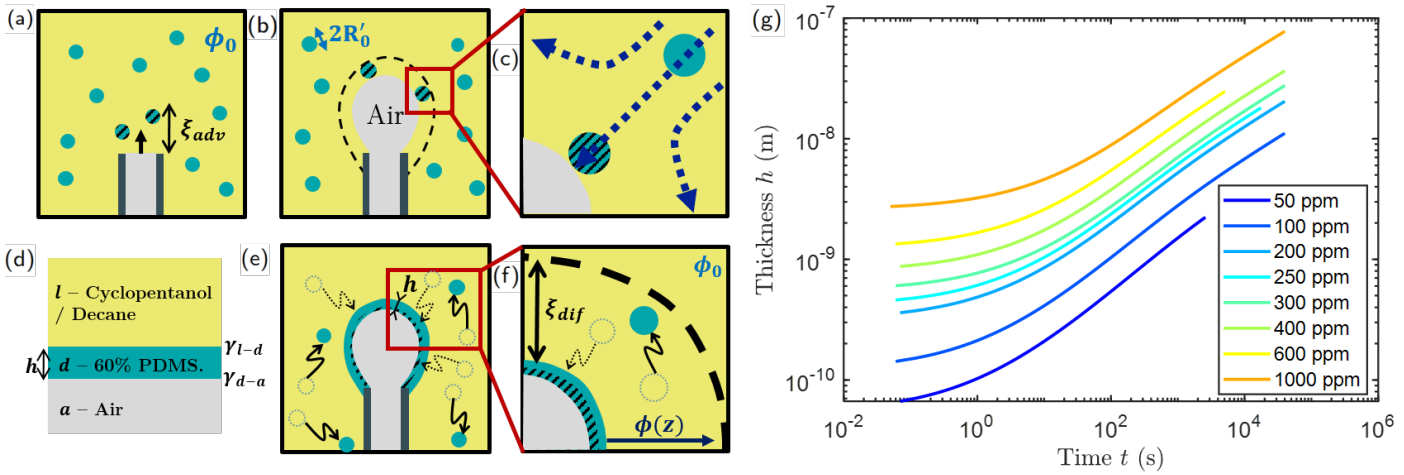

Fig. 2: Schematic representation of the transport of droplets to the air/oil interface. We emphasise that the scheme is not to scale: the bubble radius is about 1000 μm whereas the droplet radius does not exceed 2 μm a) Before and b) During bubble swelling. Hatched droplets are advected towards the interface during swelling. R'_0 is the droplet radius at time $t = 0$ when the tensiometry measurement starts. c) Enlarged view showing two droplets in the reference frame of the bubble interface. They are subjected to the flow created by bubble swelling. The hatched droplet will coalesce with the interface. d) Zoom on the different layers. e) Droplets uptake due to Brownian motion. f) Enlarged view: droplets that diffuse toward the interface and within the depletion layer ξ_{dif} are uptaken. g) Thickness h as a function of time computed using Eq. 12 for different concentrations in PDMS (in ppm).

swelling, to a distance $d_e = d_i S_i/S_e$, where S_i and S_e are the initial and final areas of the air interface. During bubble swelling, a droplet experiences a collision with the interface if located at distance $d_e = R'_0$, the droplet radius. Before swelling, these droplets are located at a distance $\xi_{adv} = \alpha d_i$ from the interface, where α is a numerical factor of order unity accounting for the difference between the trajectories of fluid particles and microdroplets. Capture hence occurs within a volume of emulsion $\xi_{adv} S_i = \alpha R'_0 S_e$, which corresponds to a PDMS-rich phase of volume $\alpha R'_0 S_e \phi_0$ that spreads over the bubble surface of area S_e, so that thickness h_{adv} due to advection can be written as:

$$h_{adv} = \alpha R'_0 \phi_0. \tag{6}$$

We now discuss the contribution of diffusion to the growth of the PDMS-rich layer $h_{dif}(t)$. The thickness h_{dif} corresponds to droplets located in a layer of the oil mixture of thickness $\xi_{dif} = h_{dif}/\phi$. Their transport by diffusion to the air interface involves a typical timescale $t_{dif} = \xi_{dif}^2/2D$ which we compare to the timescale for droplet growth τ_c defined in section 4 :

$$\frac{t_{dif}}{\tau_c} = \left(\frac{h_{dif}}{h^*}\right)^2, \tag{7}$$

where $h^* = R_0\sqrt{\frac{2}{3}\phi}$. For PDMS-rich layers thicker than h^*, coalescence between droplets during uptake by the interface should be taken into account. h^* is of the order of one nanometer. In the following, we offer to combine the time evolution of the droplet radius in bulk through Eq.2 with the diffusive transport of droplets to the interface. We first comment on the number density of droplets close to the interface: it decreases over the depletion layer of thickness ξ_{dif} from its bulk value to zero. The coalescence rate between droplets $1/\tau_c$ is thus smaller than in bulk. Since the rate of coalescence depends on the droplet number density through Eq.3, its approximate value in the depletion layer is given by the average number density in the depletion layer, taken to be half the bulk value. As a result, in the depletion layer, the growth rate is approximated as $\frac{1}{2\tau_c}$. Note that this factor 2 will appear as $2^{-1/6}$ in the final result, and is therefore not crucial. We then have checked that the uptake of the droplets by the interface does not significantly decrease the amount of droplets in the bulk far from the interface. Actually, the total volume of droplets is about a thousand times larger than the volume of the PDMS-rich phase at the interface.

Consequently, the droplet volume fraction $\phi(z,t)$ in the depletion layer follows a diffusion equation as a function of z, the distance to the air/oil interface and t, the time since the beginning of the tensiometry measurement:

$$\frac{\partial \phi}{\partial t} = D(t)\frac{\partial^2 \phi}{\partial z^2}, \tag{8}$$

where the time dependent diffusion coefficient $D(t)$ is computed from Eq. 4 to be:

$$D(t) = \frac{k_B T}{6\pi\eta R'_0\left(1+\frac{t}{2\tau'_c}\right)^{1/3}}. \tag{9}$$

where R'_0 is the microdroplet radius at the beginning of the tensiometry measurement computed from Eq. 2 and τ'_c is computed from Eq. 3 using R'_0 as the microdroplets radius.
The initial condition corresponds to a homogeneous fraction $\phi = \phi_0$. We substitute the variable t by τ such that $d\tau = D(t)dt$. The problem is now analogous to the classical problem of heat diffusion near an interface at constant temperature, with an initial condition of constant temperature - but different from the one of the interface[3,5]. The solution is:

$$\phi = \frac{\phi_0}{\sqrt{\pi}}\int_0^{z/\sqrt{\tau}} e^{-\frac{v^2}{4}} dv. \tag{10}$$

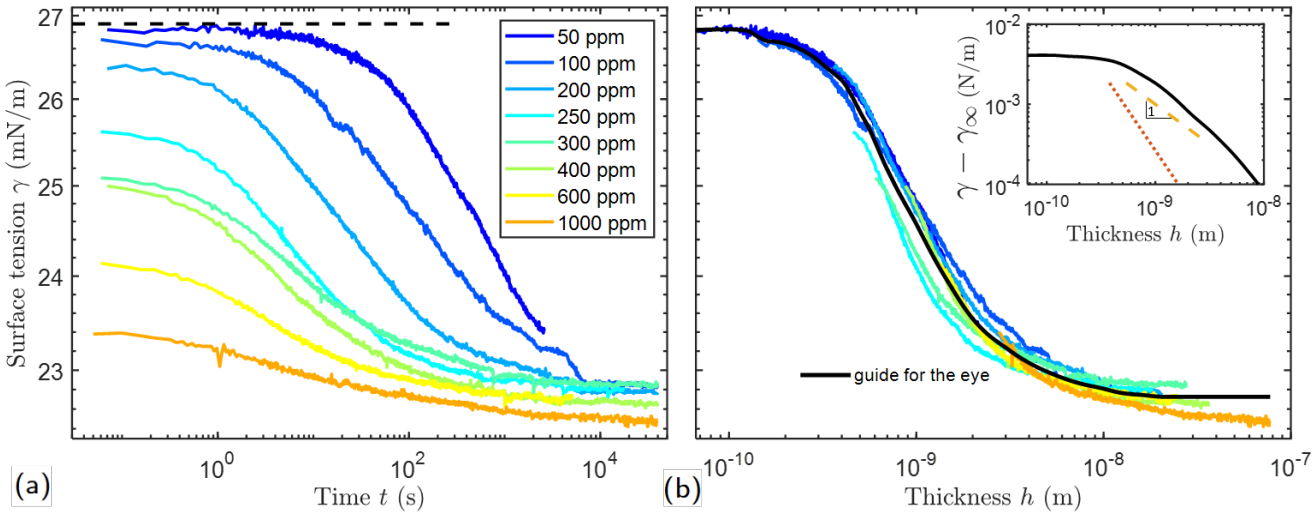

Fig. 3: (a) Surface tension as a function of time for different concentrations in PDMS. The oil mixture has a constant weight fraction in cyclopentanol of 70%. The dashed line corresponds to the surface tension of the oil mixture without PDMS. The uncertainty on surface tension is $\Delta\gamma = \pm 0.1\,\mathrm{mN/m}$ and error bars are too small to appear. (b) Same data versus thickness h as computed from Eq. 12. Inset: energy of the thin film as a function of thickness h. Dotted and dashed lines respectively show the power laws $A/12\pi h^2$ with $A = 10^{-20} J$ (red) and h^{-1} (yellow).

According to Eq. 9 and 10, the flux of the PDMS-rich phase towards the interface is $D\frac{\partial\phi}{\partial z} = D(t)\frac{\phi_0}{\sqrt{\pi\tau}}$ at $z = 0$, and the thickness of the uptaken layer is $h_{dif} = 2\phi_0\sqrt{\frac{\tau}{\pi}}$. Substituting τ by the real time variable t and using Eq. 9 yields:

$$h_{dif}(t) = 2R_0'\sqrt{\frac{\phi_0}{\pi}}\left(\left(1+\frac{t}{2\tau_c'}\right)^{2/3} - 1\right)^{1/2}. \qquad (11)$$

Finally, the total uptake of the dispersed phase as a function of time is given by:

$$h(t) = h_{adv} + h_{dif}(t). \qquad (12)$$

4.2.2 Comparison with surface tension measurements

Using Eq. 12 and $\alpha = 4$, the thickness of the PDMS-rich phase layer is computed over time in Fig. 2g. The thickness varies over a wide range: from Angström to 100 nm. We further represent the surface tension data of Fig. 3a as a function of the layer thickness in Fig. 3b. All data nicely collapses onto a master curve showing we measure the surface energy of the oil mixture at an interface with air, covered by the PDMS-rich phase. The value $\alpha = 4$ was found to result in the best collapse of the data, consistently with α being a geometrical factor.

For layers of vanishing thickness, smaller than typically 1 Å, we measure no effect of the PDMS-rich phase on the surface energy which remains equals to that of the liquid mixture without PDMS. The surface is probably only partially covered by PDMS and decane molecules, which do not significantly affect the interface energy. Interestingly, the thickness of PDMS monolayers spread on the surface of a water bath was reported to be 8 Å, independently of the polymer length[13]. This value is smaller than the Kuhn length of PDMS, 13 Å. However, it is difficult to quantitatively compare the structure of PDMS at the water surface with the one of the PDMS-rich phase at the surface of the oil mixtures we study.

Fig. 3b also shows that, for thicknesses larger than about 10 nm, the surface tension reaches a plateau, corresponding to a value of $\gamma_\infty = 22.7 \pm 0.15$ mN/m. We interpret this value as the sum of the surface tensions of the two interfaces depicted in Fig. 2d: $\gamma_{d-a} = 21.7\,\mathrm{mN/m}$ and $\gamma_{l-d} = 0.8 \pm 0.7\mathrm{mN/m}$. Hence, γ_∞ corresponds to the energy of the air/layer/oil system in which the air and oil phase (as defined in Fig. 2d) do not interact because the thickness of the PDMS-rich phase is large. At smaller thicknesses, however, these interactions have a significant contribution on the system's surface tension which increases with decreasing thickness. In the inset of Fig. 3b, we plot the surface energy of the thin film defined as $\gamma - \gamma_\infty$. We observe that the energy decreases with thickness according to a power law close to h^{-1}. We emphasise that Van der Waals interactions, for which energy decays as h^{-2}, fail to describe the surface energy we measure. In addition, using a value for the Hamaker constant of 10^{-20} J, yields Van der Waals energies that are one order of magnitude smaller than the ones we measure (see inset of Fig. 3b) . The thickness variations of the thin film energy we measure could be due to the polymeric nature of PDMS, or to the PDMS densities at both interfaces but the analysis of these effects goes beyond the scope of this study. As far as we know, the structure of thin layers of PDMS has never been studied in similar oil systems as the one we probe.

We now focus on the behaviour of droplets at the air/oil interface. Our analysis suggests that there is no delay for the uptake by the air/oil interface. This indicates that there is no significant energy barrier for the droplets to enter this interface. This is consistent with the values of the refractive indexes n_i of the different fluids (see the Supplementary Information†) that verify $n_a < n_d < n_l$. When a droplet reaches the interface, a thin film of decane/cyclopentanol mixture (l) is entrapped between the droplet (d) and air (a). The Hamaker constant of this system is proportional to $(n_d^2 - n_a^2)(n_l^2 - n_a^2)$ [10], and is therefore positive; as a result, the oil film is unstable and the entry of droplets at

the air/oil interface is favoured. In contrast, the PDMS-rich film sandwiched between air and the oil mixture is stable. This is different from aqueous solution in which the entry of antifoam droplets at the air interface can be hindered by the presence of surfactants, which result in large entry barriers as described in the literature[6,8].

5 Conclusions

Taking advantage of a spontaneous emulsification process in a ternary oil mixture (PDMS, decane and cyclopentanol), we obtain controlled emulsions that separate into two phases, the dispersed phase mostly containing PDMS. The growth kinetics of the spontaneously formed droplets were measured and successfully described using a non-delayed coalescence model driven by Brownian diffusion.

When a bubble is freshly created in these emulsions, using simple tensiometry measurements, we demonstrate that PDMS-rich droplets enter the air/oil interface and spread over it, thereby forming a thin film. The transfer of the PDMS-rich phase from the bulk emulsion to the air interface is successfully analysed using an advection-diffusion model. Our analysis culminates in the measurement of the surface energy of the PDMS-rich phase thin film trapped between air and oil as a function of its thickness. PDMS being widely used as an antifoam, the transport phenomena occurring at air interfaces created in oil-in-oil emulsions are of particular interest to understand the foaming properties of oil mixtures.

Conflicts of interest

There are no conflicts to declare.

Notes and references

1 Bergeron, V., Cooper, P., Fischer, C., Giermanska-Kahn, J., Langevin, D., and Pouchelon, A. Polydimethylsiloxane (PDMS)-based antifoams. *Colloids and Surfaces A: Physicochemical and Engineering Aspects 122*, 1 (Apr. 1997), 103–120.

2 Binder, K., and Stauffer, D. Theory for the Slowing Down of the Relaxation and Spinodal Decomposition of Binary Mixtures. *Physical Review Letters 33*, 17 (Oct. 1974), 1006–1009.

3 Carslaw, H. S., and Jaeger, J. C. *Conduction of heat in solids*, 2. ed ed. Clarendon, Oxford, 1980.

4 Chandran Suja, V., Kar, A., Cates, W., Remmert, S. M., and Fuller, G. G. Foam stability in filtered lubricants containing antifoams. *Journal of Colloid and Interface Science 567* (May 2020), 1–9.

5 Crank, J. *The mathematics of diffusion*, 2. ed., repr ed. Univ. Pr, Oxford, 2011.

6 Denkov, N. D. Mechanisms of foam destruction by oil-based antifoams. *Langmuir: the ACS journal of surfaces and colloids 20*, 22 (Oct. 2004), 9463–9505.

7 Garrett, P., Davis, J., and Rendall, H. An experimental study of the antifoam behaviour of mixtures of a hydrocarbon oil and hydrophobic particles. *Colloids and Surfaces A: Physicochemical and Engineering Aspects 85*, 2-3 (June 1994), 159–197.

8 Hadjiiski, A., Tcholakova, S., Ivanov, I. B., Gurkov, T. D., and Leonard, E. F. Gentle Film Trapping Technique with Application to Drop Entry Measurements. *Langmuir 18*, 1 (Jan. 2002), 127–138. Publisher: American Chemical Society.

9 Horozov, T. S. Foams and foam films stabilised by solid particles. *Current Opinion in Colloid & Interface Science 13*, 3 (June 2008), 134–140.

10 Israelachvili, J. N. *Intermolecular and surface forces*. Academic Press, London, 1992. OCLC: 137313926.

11 Kabal'nov, A. S., Pertzov, A. V., and Shchukin, E. D. Ostwald ripening in two-component disperse phase systems: Application to emulsion stability. *Colloids and Surfaces 24*, 1 (May 1987), 19–32.

12 Koczo, K., Koczone, J. K., and Wasan, D. T. Mechanisms for Antifoaming Action in Aqueous Systems by Hydrophobic Particles and Insoluble Liquids. *Journal of Colloid and Interface Science 166*, 1 (Aug. 1994), 225–238.

13 Lee, L. T., Mann, E. K., Langevin, D., and Farnoux, B. Neutron reflectivity and ellipsometry studies of a polymer molecular layer spread on the water surface. *Langmuir 7*, 12 (Dec. 1991), 3076–3080.

14 Liu, D., Mahmood, A., Weng, D., and Wang, J. Life-Like Motion of Oil Drops at the Air–Liquid Interface. *Langmuir 35*, 49 (Dec. 2019), 16146–16152.

15 Mensire, R. *Hydrodynamics of oil in contact with an aqueous foam : wetting, imbibition dynamics and flow in rough confined media*. PhD thesis, Sept. 2016.

16 Mensire, R., and Lorenceau, E. Stable oil-laden foams: Formation and evolution. *Advances in Colloid and Interface Science 247* (Sept. 2017), 465–476.

17 Provencher, S. W. A constrained regularization method for inverting data represented by linear algebraic or integral equations. *Computer Physics Communications 27*, 3 (Sept. 1982), 213–227.

18 Pu, W., Wei, P., Sun, L., Pu, Y., and Chen, Y. Investigation on stabilization of foam in the presence of crude oil for improved oil recovery. *Journal of Dispersion Science and Technology 40*, 5 (May 2019), 646–656. Publisher: Taylor & Francis _eprint: https://doi.org/10.1080/01932691.2018.1476153.

19 Pugh, R. J. *Bubble and Foam Chemistry*. Cambridge University Press, Cambridge, 2016.

20 Salonen, A., Langevin, D., and Perrin, P. Light and temperature bi-responsive emulsion foams. *Soft Matter 6*, 21 (Nov. 2010), 5308–5311. Publisher: The Royal Society of Chemistry.

21 Schneider, M., Zou, Z., Langevin, D., and Salonen, A. Foamed emulsion drainage: flow and trapping of drops. *Soft Matter 13*, 22 (June 2017), 4132–4141. Publisher: The Royal Society of Chemistry.

22 Shabani, R., Kumar, R., and Cho, H. J. Droplets on liquid surfaces: Dual equilibrium states and their energy barrier. *Applied Physics Letters 102*, 18 (May 2013), 184101.

23 SIGGIA, E. D. Late stages of spinodal decomposition in binary mixtures. *Physical Review A 20*, 2 (Aug. 1979), 595–605.

24 SITNIKOVA, N. L., SPRIK, R., WEGDAM, G., AND EISER, E. Spontaneously Formed trans-Anethol/Water/Alcohol Emulsions: Mechanism of Formation and Stability. *Langmuir 21*, 16 (Aug. 2005), 7083–7089. Publisher: American Chemical Society.